euspen's 23rd International Conference & Exhibition, Copenhagen, DK, June 2023
www.euspen.eu

Active disturbance rejection based on periodic disturbance estimator for machine tools

Anna-Carina Kurth[1], Thomas Gorius[1]

[1]*Carl Zeiss SMT GmbH, Oberkochen, Baden-Württemberg, Germany*

anna-carina.kurth@zeiss.com

Abstract
Machine tools are for machining a workpiece by a tool. The main components of machine tools are the frame, the power unit, the control and the steering. The position of the tool should be stabilized at the zero position by the control, which is typically a pure feedback control. The power unit realizes the movement of the workpiece. Thereby, large accelerations of the workpiece must be realized in order to increase the economic efficiency. The periodic movement of the workpiece respectively the power unit excites the entire machine tool and ultimately the tool itself resulting in a position error signal containing the frequencies from the movement. Since the motion pattern of the workpiece is customer knowledge, the frequencies it contains are not known in advance. Additionally, the frequencies change over time due to different motion patterns. However, the range in which the frequencies lie is known. In high-precision positioning of machine tools, there are three possibilities to reduce position errors of the tool: reduction of the disturbance causing the errors, optimization of the plant, which is the whole machine tool, or the control. This contribution focuses on the optimization of the control. By adding active disturbance rejection to the existing feedback controller for the tool, the influence of the disturbance on the position error of the tool is reduced. The resulting controller contains a disturbance estimator based on a Kalman filter. Hereby, the system, which shall be estimated, is either modelled as MIMO system or as a decoupled SISO system. A comparison between the SISO and MIMO realization leads to opposing requirements regarding the parameter tuning and the performance. However, the controller reduces the position error in both cases drastically even under the influence of sensor noise and mismatches between the plant and the system included in the filter.
In summary, our approach permits us to estimate disturbances evolving from periodic movements of the workpiece and reduce their impact on the position error signal of the tool. This reduction translates directly into improved machine tool overall performance.

Disturbance Estimation, Kalman Filter, Observability Analysis, Active Disturbance Rejection

1. Introduction

Increasing demands on the accuracy of components in manufacturing, increase the demand on the positioning accuracy of machine tools. Here, not only the design of machine tools and their main components- frames, power unit and steering- plays a major role, but especially its control in order to compensate for disturbances [1]. The goal of the control is to stabilize the zero position of the tool center point (TCP), which represents the contact point between the tool and the workpiece. For this purpose, the position of the TCP is measured and corrected by the change in position of the tool. Typically, pure feedback controllers are used as a first approach [1].

The disturbances may originate, for example, in moving parts of the machine tool itself like the power unit and cannot be sufficiently damped on the way to the TCP or they may arise externally. Therefore, even with a perfectly decoupled machine, external disturbances would cause positioning inaccuracies that can only be compensated for by control. Depending on the characteristics and the origin of the disturbances, different types of control can be considered, which optimize the existing feedback control [2].

This paper focuses on disturbances caused by a periodically moving part of the machine tool itself like the power unit. This part moves over a certain period of time with a motion pattern, which is characterized by certain frequencies. After this period, the pattern changes and thus also the frequencies contained in the movement spectrum. Since the motion pattern of the workpiece is customer knowledge, the frequencies it contains are not known in advance. However, the propagation of the disturbance through the machine tool results in the disturbance arriving at the TCP damped, but containing the same frequencies of the motion pattern. These frequencies can now be seen in the position error signal of the TCP, which is given in all six degrees of freedom (DoF). Therefore, this signal can be used to estimate the disturbance acting on the machine tool. This disturbance is subsequently used in a feedforward control to compensate its effect on the systems performance.

The estimate of a disturbance can be calculated by a variety of methods. One widely used method is to set up the extended system dynamics so that the disturbance is now considered as a system state that can be calculated using observer concepts from classical control engineering. These include, for example, Luenberger observers or Kalman filters [3]. We concentrate on Kalman filters in this contribution, since they are by concept more robust to measurement and process noise as well as model uncertainties than Luenberger observers.

In [4] a good overview of control methodologies for machine tools can be found. However, it lacks of an active disturbance rejection based on a periodic disturbance estimator.

The remaining paper is structured as follows: First, section 2 discusses in more detail the problem and the basics for solving it. Then, in section 3, the simulations and their results are presented, which are carried out to validate the concept. The performance of the approach is evaluated based on two criteria.

Finally, section 4 deals with the conclusion and further work that is planned.

2. Problem Statement

This section describes the basics needed to design a Kalman filter used to estimate the periodic disturbance arising due to moving parts of the machine tool.

2.1. Modelling of the plant

The tool of the machine tool is modelled via FEM and connected to additional models displaying the frames, the steering and the power unit. The model of the tool contains a high number of states. This model is reduced by balanced truncation, see for example [5], such that a time-continuous system

$$\begin{aligned} \dot{\boldsymbol{x}} &= \boldsymbol{Ax} + \boldsymbol{Bu} + \boldsymbol{Ed}, \qquad \boldsymbol{x}(\boldsymbol{0}) = \boldsymbol{x_0} \\ \boldsymbol{y} &= \boldsymbol{Cx} + \boldsymbol{Du} \end{aligned} \tag{1}$$

with twelve states $\boldsymbol{x}(t) \in \mathbb{R}^{\boldsymbol{12}}$ arises. The physical motivation behind the number of states are two states for each DoF, which result from the interpretation as a mechanical system

$$m\ddot{\vartheta} + k\vartheta = F \tag{2}$$

for each DoF with some mass m, stiffness k, input force F, acceleration $\ddot{\vartheta}$ and position ϑ [2]. With the input $\boldsymbol{u}(t) \in \mathbb{R}^{\boldsymbol{6}}$ the position as well as the orientation of the TCP is controllable in six DoF. The disturbance $\boldsymbol{d}(t) \in \mathbb{R}^{\boldsymbol{6}}$ results through a periodically moving part of the machine tool like the power unit. Lastly, the output $\boldsymbol{y}(t) \in \mathbb{R}^{\boldsymbol{6}}$ is the position and orientation of the TCP measured in six DoF. The dimensions of the dynamic matrix $\boldsymbol{A} \in \mathbb{R}^{\boldsymbol{12\times12}}$, the input matrix $\boldsymbol{B} \in \mathbb{R}^{\boldsymbol{12\times6}}$, the disturbance matrix $\boldsymbol{E} \in \mathbb{R}^{\boldsymbol{12\times6}}$, the output matrix $\boldsymbol{C} \in \mathbb{R}^{\boldsymbol{6\times12}}$ and the feedthrough matrix $\boldsymbol{D} \in \mathbb{R}^{\boldsymbol{6\times6}}$ are accordingly.

If an assumption can be made about the model of the disturbance, the extended system dynamics can be set up

$$\begin{aligned} \begin{bmatrix} \dot{\boldsymbol{x}}(\boldsymbol{t}) \\ \dot{\boldsymbol{z}}(\boldsymbol{t}) \end{bmatrix} &= \begin{bmatrix} \boldsymbol{A} & \boldsymbol{EG} \\ \boldsymbol{0} & \boldsymbol{M} \end{bmatrix} \begin{bmatrix} \boldsymbol{x}(\boldsymbol{t}) \\ \boldsymbol{z}(\boldsymbol{t}) \end{bmatrix} + \begin{bmatrix} \boldsymbol{B} \\ \boldsymbol{0} \end{bmatrix} \boldsymbol{u}, \qquad \begin{bmatrix} \boldsymbol{x}(\boldsymbol{0}) \\ \boldsymbol{z}(\boldsymbol{0}) \end{bmatrix} = \begin{bmatrix} \boldsymbol{x_0} \\ \boldsymbol{z_0} \end{bmatrix} \\ \boldsymbol{y}(\boldsymbol{t}) &= [\boldsymbol{C} \quad \boldsymbol{0}] \begin{bmatrix} \boldsymbol{x}(\boldsymbol{t}) \\ \boldsymbol{z}(\boldsymbol{t}) \end{bmatrix} + \boldsymbol{Du} \end{aligned} \tag{3}$$

containing additional states $\boldsymbol{z}(t) \in \mathbb{R}^{\boldsymbol{n}}$ needed for the dynamic description of the disturbance $\boldsymbol{d}$. Its dynamics is given by the dynamic matrix $\boldsymbol{M} \in \mathbb{R}^{\boldsymbol{n\times n}}$, which is determined later. Hereby, the dimension n depends on the characteristics of the disturbance $\boldsymbol{d}$. The matrix $\boldsymbol{G} \in \mathbb{R}^{\boldsymbol{6\times n}}$ is to be defined and selects the states $\boldsymbol{z}$ describing the disturbance $\boldsymbol{d}$.

2.2. Modelling of the disturbance

The disturbance is modelled as a multisine due to the basics of fourier transformation that every periodical signal can be displayed as an infinite sum of sine functions. The state-space model of a representative sinusoidal disturbance model with frequency ω_i is given by

$$\begin{aligned} \dot{\boldsymbol{z}}_{\boldsymbol{i}}(\boldsymbol{t}) &= \boldsymbol{M_i z_i}(\boldsymbol{t}) := \begin{bmatrix} 0 & 1 \\ -\omega_i^2 & 0 \end{bmatrix} \boldsymbol{z_i}(\boldsymbol{t}), \\ \boldsymbol{z_i}(0) &= \begin{bmatrix} a_i sin(\varphi_i) \\ a_i\omega_i cos(\varphi_i) \end{bmatrix}, \end{aligned} \tag{4}$$

where the amplitude a_i and the phase shift φ_i determine the initial condition. A certain number of state-spaces of this form is added such that the disturbance

$$\boldsymbol{d}(\boldsymbol{t}) = \boldsymbol{Gz}(\boldsymbol{t}) := \sum_{\boldsymbol{i=0}}^{\frac{\boldsymbol{n}}{\boldsymbol{2}}-\boldsymbol{1}} \boldsymbol{z_{2i+1}}(\boldsymbol{t}) \tag{5}$$

is generated approximately. Only for $n \to \infty$ every periodic signal could be generated exactly. The matrix $\boldsymbol{M}$ is a block diagonal matrix, with the matrices $\boldsymbol{M_i}$ on the diagonal.

The assumption is made that the disturbance acts as an additional input disturbance. Therefore, it enters the system through the input matrix and the equality $\boldsymbol{E} = \boldsymbol{B}$ in (1) holds.

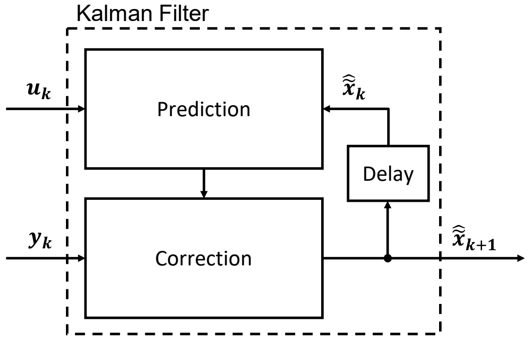

Figure 1*. Scheme of the Kalman filter. The prediction step uses the control input as well as the result of the previous correction step. In the correction step, the current measurement and the result of the prediction step is used to estimate the states.*

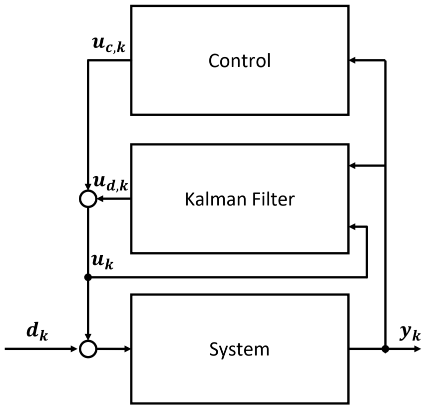

Figure 2. *Overall control structure. The system has as Input the control output consisting of the feedback control and the feedforward control generated in the Kalman filter. Additionally, the disturbance enters the system as input disturbance.*

2.3. Kalman Filter

A Kalman filer is an estimator observing not measurable states of a system while reducing measurement noise for measurable states. For implementation the system is discretized with respect to time with a sample rate of 2 kHz. Hereby, the time-discrete systems

$$\begin{aligned} \begin{bmatrix} \bar{\boldsymbol{x}}_{\boldsymbol{k+1}} \\ \bar{\boldsymbol{z}}_{\boldsymbol{k+1}} \end{bmatrix} &= \begin{bmatrix} \boldsymbol{I} + \bar{\boldsymbol{A}}h & \bar{\boldsymbol{B}}\boldsymbol{G}h \\ \boldsymbol{0} & \boldsymbol{I} + \boldsymbol{M}h \end{bmatrix} \begin{bmatrix} \bar{\boldsymbol{x}}_{\boldsymbol{k}} \\ \bar{\boldsymbol{z}}_{\boldsymbol{k}} \end{bmatrix} + \begin{bmatrix} \bar{\boldsymbol{B}}h \\ \boldsymbol{0} \end{bmatrix} \boldsymbol{u_k} + \boldsymbol{v_k} \\ &= \tilde{\boldsymbol{A}}\tilde{\boldsymbol{x}}_{\boldsymbol{k}} + \tilde{\boldsymbol{B}}\boldsymbol{u_k} + \boldsymbol{v_k} \\ \bar{\boldsymbol{y}}_{\boldsymbol{k}} &= [\bar{\boldsymbol{C}}h \quad \boldsymbol{0}] \begin{bmatrix} \bar{\boldsymbol{x}}_{\boldsymbol{k}} \\ \bar{\boldsymbol{z}}_{\boldsymbol{k}} \end{bmatrix} + \bar{\boldsymbol{D}}h\boldsymbol{u_k} + \boldsymbol{w_k} \\ &= \tilde{\boldsymbol{C}}\tilde{\boldsymbol{x}}_{\boldsymbol{k}} + \tilde{\boldsymbol{D}}\boldsymbol{u_k} + \boldsymbol{w_k} \end{aligned} \tag{6}$$

generated from (3) and (4) should be observed. The bar denotes that the the model in the Kalman filter may vary from the actual model due to modelling uncertainties. However, the matrices belonging to the model of the disturbance are already an assumption. Hereby, $h = 0.5$ ms is the sample time, $\bar{\boldsymbol{x}}_{\boldsymbol{k}} = \bar{\boldsymbol{x}}(kh)$ the state at time $t = kh$, $\boldsymbol{v_k}$ is the process noise and $\boldsymbol{w_k}$ is the measurement noise. The noise has to be uniformly distributed.

The concept of the Kalman filter includes two steps: the prediction and the correction step.

The prediction step estimates the states in the next time step based on the system dynamics. The calculation rule

$$\begin{aligned} \hat{\tilde{\boldsymbol{x}}}_{k+1|k} &= \tilde{\mathbf{A}}\hat{\tilde{\boldsymbol{x}}}_{k|k} + \tilde{\boldsymbol{B}}\boldsymbol{u_k} \\ \boldsymbol{P}_{k+1|k} &= \tilde{\boldsymbol{A}}\boldsymbol{P_{k|k}}\tilde{\boldsymbol{A}}^{\mathrm{T}} + \boldsymbol{Q} \end{aligned} \tag{7}$$

includes the estimated states denoted by the hat. The first index describes for which time step the estimation is calculated while the second index denotes the time step at which the estimation is performed. Hence, these calculations determine the states at the time step $t = (k+1)h$ using the data from the time step $t = kh$. The covariance matrix $\boldsymbol{P}$ displays the certainty for the prediction. Its initial condition is a design parameter, which is automatically chosen by Simulink. The matrix $\boldsymbol{Q}$ describes the covariance matrix of the process noise.

In the correction step, the prediction is corrected by a measurement. Therefore,

$$\begin{aligned} \boldsymbol{K}_{k+1} &= \boldsymbol{P}_{k+1|k}\widetilde{\boldsymbol{C}}^T\left(\widetilde{\boldsymbol{C}}\boldsymbol{P}_{k+1|k}\widetilde{\boldsymbol{C}}^T + \boldsymbol{R}\right)^{-1} \\ \widehat{\widetilde{\boldsymbol{x}}}_{k+1} &= \widehat{\widetilde{\boldsymbol{x}}}_{k+1|k} + \boldsymbol{K}_k\left(\boldsymbol{y}_k - \widetilde{\boldsymbol{C}}_k\widehat{\widetilde{\boldsymbol{x}}}_{l+1|k}\right) \\ \boldsymbol{P}_{k+1} &= \left(\boldsymbol{I} - \boldsymbol{K}_{k+1}\widetilde{\boldsymbol{C}}\right)\boldsymbol{P}_{k+1|k}. \end{aligned} \qquad (8)$$

Hereby, $\boldsymbol{K}_{k+1}$ is the so called Kalman gain and the matrix $\boldsymbol{R}$ is the covariance matrix of the measurement noise. The block diagram in **Figure 1** shows the structure of the Kalman Filter.

The representation of the Kalman filter is valid for SISO as well as MIMO systems.

2.4. Control Structure

The input $\boldsymbol{u_k} = \boldsymbol{u}_{c,k} + \boldsymbol{u}_{d,k}$ contains two parts: the feedback and the feedforward control. The feedback control $\boldsymbol{u}_{c,k}$ is assumed to be a PID-controller combined with a decoupling matrix. However the methodology is independent of the type of controller. The decoupling is based on a frequency approach (rigid body decoupling) and works well for a certain frequency range, in which the system behaves as a rigid body. Besides this range, the system acts as a flexible body and is therefore not necessarily decoupled. However, in the relevant frequency range for the considered evaluations in this contribution, this assumption is valid.

The feedforward control $\boldsymbol{u}_{d,k} = -[\boldsymbol{0} \quad \boldsymbol{G}]\widehat{\widetilde{\boldsymbol{x}}}_k$ uses the results from the Kalman filter and contains the estimated states corresponding to the disturbance. It can be activated and deactivated to investigate the impact of using this control.

The overall control structure is displayed in **Figure 2**.

3. Simulations

The plant used in the simulations is the one obtained from balanced truncation, see (1). The model in the Kalman filter differs from this one such that the influence of model uncertainties can be observed. Two different approaches are considered. In both cases the feedback control is tuned such that the bandwidth is around 150Hz and the sample time is 20kHz. Amplitude and phase of the disturbance are randomly generated with 15 fixed frequencies between 18-100Hz. The pattern changes after three seconds. Between 3 and 3.1 seconds the first motion pattern is ramped down. Starting at 3.1 seconds until 3.2 seconds the second motion pattern is ramped up. Afterwards the second motion pattern is active. Hence, the influence of changing motion patterns and the convergence of the Kalman filter can be investigated. The results are transferable to lower sample rates and bandwidths, if the disturbance is more low-frequent.

3.1. SISO

First, it is assumed that the decoupling of the system works well, so that there are six decoupled SISO systems, each with system and input matrix

$$\overline{\boldsymbol{A}}_i = \begin{bmatrix} 0 & 1 \\ -\dfrac{k_i}{m_i} & 0 \end{bmatrix}, \quad \overline{\boldsymbol{B}}_i = \begin{bmatrix} 0 \\ \dfrac{1}{m_i} \end{bmatrix}, \quad \overline{\boldsymbol{C}}_i = [1 \quad 0], \quad \overline{\boldsymbol{D}}_i = 0 \qquad (9)$$

with some mass m_i and some stiffness k_i.

For each of these systems a separate SISO Kalman filter is now designed using matrices (9) observing the disturbance in one direction. For the disturbance model in the Kalman Filter three different frequencies are incorporated, namely 10Hz , 50Hz and 100Hz. Hence, the matrix Q, see (7) has dimension 8×8 and is chosen as a diagonal matrix. The matrix R is a scalar. For the force directions the matrices are all the same, as well as for the torque directions. The covariance matrices are tuned by hand. Therefore, for each, the force axes and for the torque axes, nine degrees of freedom are available and for the whole system eighteen.

The results are displayed in **Figure 3** for a certain, hand-tuned set of design parameters. On the left side of the figure are the errors between the position of the TCP and the desired position, which is zero. Only the errors of the translational directions are displayed, but the rotational directions look similar. In grey is the signal, if the feedforward control is not activated and therefore only feedback compensation of the disturbance is incorporated. In dark blue are the signals, if the feedforward control is active. Hence, the feedforward control can reduce the error signal significantly. The change of the motion pattern does not change this statement. On the right side of **Figure 3** are the real (dark blue) as well as the estimated disturbances (light blue) in translational directions displayed. The disturbance is estimated correctly independent of the change of the motion pattern. The convergence of the Kalman Filter is therefore fast enough to estimate changing patterns. In **Figure 4** are the fast Fourier-transformed (FFT) error signals displayed. In grey is again the signal if the feedforward control is passive, while in dark blue it is active. The damping of the incorporated frequencies works especially well, but also frequencies nearby are sufficiently damped. Here, the rotational signals are neglected, too.

3.2. MIMO

In the other case, the MIMO system is used, such that

$$\overline{\boldsymbol{A}} = \boldsymbol{A}, \qquad \overline{\boldsymbol{B}} = \boldsymbol{B}, \qquad \overline{\boldsymbol{C}} = \boldsymbol{C}, \qquad \overline{\boldsymbol{D}} = \boldsymbol{D} \qquad (10)$$

holds.Hereby, also three different frequencies are contained in the disturbance. Therefore, the matrix Q has dimension 48×48 and R 6×6 leading to 54 degrees of freedom. The matrices are also tuned by hand.

The performance looks similar as in the SISO-case in **Figure 3**. Therefore, an additional figure is not displayed.

3.3.Performance Criteria

Two difference criteria are calculated to evaluate the performance of the Kalman Filters. One is the maximum error between the position of the TCP and the desired position

$$\max_{\tau \in [0,T]} e(\tau), \qquad (11)$$

while the other one is the root-mean-square error (RMSE) defined as

$$RMSE = \frac{\sqrt{\int_0^T e(\tau) d\tau}}{T}. \qquad (122)$$

The RMSE is incorporated to take the periodical characteristics of the signal into account. The results for the SISO- as well as for the MIMO-case are displayed in **Table 1**. Hereby, only the improvement is shown. The improvement factor is calculated with respect to the szenario without the feedforward control.

The SISO-Case shows higher improvements than the MIMO-case. One reason for that are the lower number of parameters that need to be tuned in the covariance matrices. However, both scenarios show the potential of the methodology presented in this contribution.

4. Conclusion and future work

In this contribution a methodology was presented to estimate a periodic disturbance measured in the position error of the TCP of a machine tool using a Kalman filter.

First, the problem statement was explained. This included the modelling of the plant. By balanced truncation, a physically motivated system with twelve states is generated from a FEM-model. This is supplemented by a model of the input disturbance so that the extended system dynamics result. The Kalman filter uses the temporally discretized model as model for the prediction step either as six SISO-models or as one MIMO- model. Measurement of the position of the TCP are used to correct the prediction. The feedback control used is a PID-controller that decouples the system in a certain frequency band and controls the system with a bandwidth of 150 Hz. In addition, the control contains a feedforward control based on the signals from the Kalman filter. By using the feedforward control, the maximum absolute position error as well as the RMSE of the TCP can be drastically minimized. The improvement potential is greater than 80% in all directions for the SISO- as well as the MIMO-case. Thus, the methodology presented here offers great potential to increase the positioning accuracy of the TCP and hence improve the overall machine tool performance. In future work, the findings shall be confirmed by measurements.

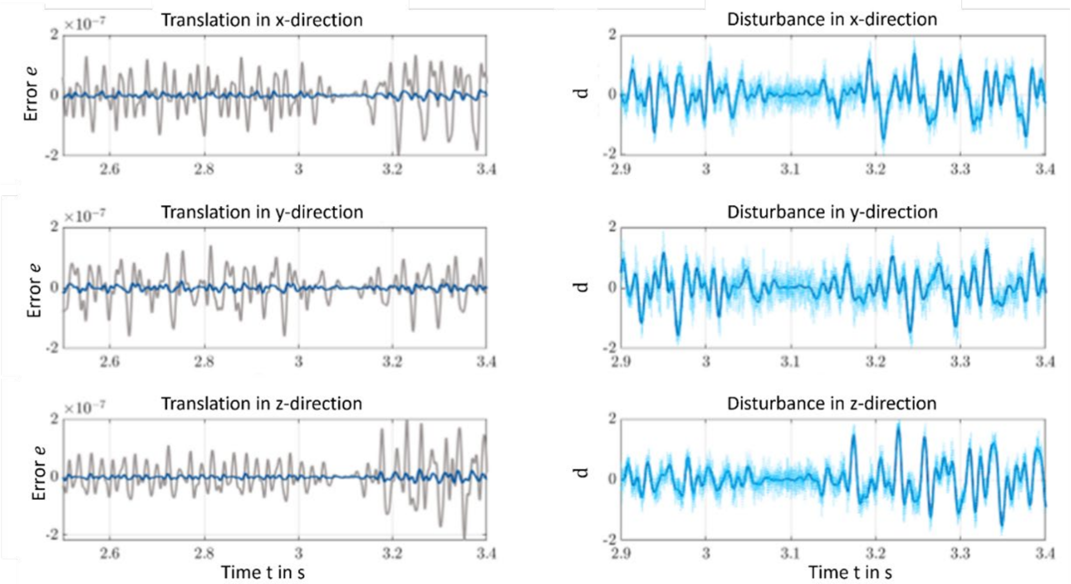

Figure 3*. Output error, disturbance and estimation of the disturbance with and without feedforward control. On the left side are the translational output errors displayed with passive (grey) and active (dark blue) feedforward control. The feedforward control leads to a reduction of the error signal. On the right side of the figure is the real disturbance (dark blue) as well as the estimated disturbance (light blue) displayed. The disturbance is estimated correctly by the Kalman filter.*

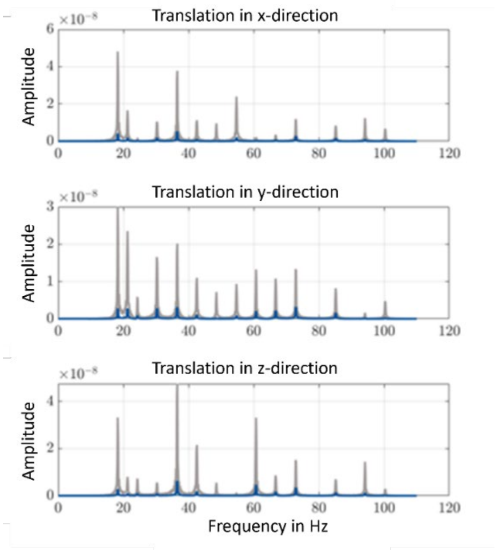

Figure 4*. FFT from the output error. In grey is the amplitude of the output error resulting without feedforward control displayed, while the dark blue signal shows the case of active feedforward control. The frequencies contained in the Kalman filter are damped the most, but also the other frequencies are damped.*

Table 1 Improvement in performance criteria for SISO- and MIMO-case.

Case	Direction	**Improvement max. error in %**	**Improvement RMSE in %**
SISO	x	88.1	88.6
	y	85.7	86.0
	z	86.3	87.3
	rx	85.5	87.0
	ry	83.3	85.5
	rz	84.8	86.1
MIMO	x	83.0	83.4
	y	84.0	83.7
	z	84.2	85.2
	rx	83.6	82.9
	ry	81.2	82.1
	rz	80.3	81.5

References

[1] Kim D, Kim S 1996 An Iterative Learning Control Method with Application for CNC Machine Tools *IEEE Transactions on industrial applications* **32** 66-72

[2] Subrahmanyan P K and Trumper D L 2000 Synthesis of Passive Vibration Isolation Mounts for Machine Tools – A Control Systems Paradigm *Proceedings of the American Control Conference, Chicago, Illinois* 2886-2891.

[3] Zhang Y, Zhao Z, Lu T, Yuan L, Xu W, Zhu J 2009 A Comparative Study of Luenberger Observer, Sliding Mode Observer and Extended Kalman Filter for Sensorless Vector Control of Induction Motor Drives *IEEE Enegry Conversion Congress and Exposition*

[4] Koren Y 1997 Control of Machine Tools *Journal of Manufacturing Science and Engineering* **119** 749-755

[5] Gugercin S and Antoulas A C 2007 A Survey of Model Reduction by Balanced Truncation and Some New Results *International Journal of Control* **77** 748-766